Macromolecules

ARTICLE

pubs.acs.org/Macromolecules

"Arm-First" Synthesis of Core-Cross-Linked Multiarm Star Polyethylenes by Coupling Palladium-Catalyzed Ethylene "Living" Polymerization with Atom-Transfer Radical Polymerization

Pingwei Liu,[†,‡] Eric Landry,[†] Zhibin Ye,[†,§,*] Helen Joly,[§] Wen-Jun Wang,[‡,*] and Bo-Geng Li[‡]

[†]School of Engineering, Laurentian University, Sudbury, Ontario P3E 2C6, Canada

[‡]State Key Lab of Chemical Engineering, Institute of Polymerization and Polymer Engineering, Department of Chemical and Biological Engineering, Zhejiang University, Hangzhou, 310027, China

[§]Department of Chemistry and Biochemistry, Laurentian University, Sudbury, Ontario P3E 2C6, Canada

Supporting Information

ABSTRACT: We report in this article the "arm-first" synthesis of core−shell-structured multiarm polyethylene (PE) star polymers having multiple linear-but-branched PE arms joined at a cross-linked polydivinylbenzene (polyDVB) core. This synthesis is achieved in two steps by coupling two mechanistically incompatible polymerization techniques, Pd-catalyzed coordinative ethylene "living" polymerization and atom-transfer radical polymerization (ATRP). Ethylene "living" polymerization was first carried out using a functionalized Pd−diimine catalyst, $[(ArN{=}C(Me){-}(Me)C{=}NAr)Pd(CH_2)_3C(O)O(CH_2)_2OC(O)C(CH_3)_2Br]^+SbF_6^-$ (Ar = 2,6-$(iPr)_2C_6H_3$) (**1**), to directly synthesize narrow-distributed PE macroinitiators (MIs) containing an end-capping 2-bromoisobutyryl group active for initiating ATRP. Featured with controllable molecular weights at low polydispersity, the PE MIs are employed subsequently in the second step to initiate cross-linking polymerization of divinylbenzene (DVB) via ATRP to obtain the core-cross-linked star polymers. As a demonstration, three PE MIs at different lengths (number-average molecular weight of 7.3, 10.3, and 13.7 kg/mol, respectively) were specifically synthesized and employed for star construction. In the ATRP step, the effects of the various polymerization parameters, including MI concentration, the molar ratio of DVB to MI, and MI length, on the polymerization kinetics, star yield, average arm number, and average molecular weights of the star polymers were investigated systematically. By controlling the polymerization parameters, a range of PE star polymers having narrow-distributed arm lengths (7.3−13.7 kg/mol) and controllable average arm numbers (ca. 5−43 per star) have thus been successfully synthesized. A study on dilution solution properties of these star polymers having various structural parameters reveals their spherical chain conformation and resemblance of rigid spheres and high-generation dendrimers, with their intrinsic viscosity depending primarily on arm length while not on arm number or polymer molecular weight.

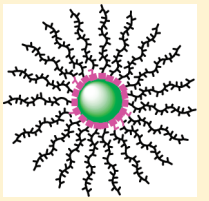

INTRODUCTION

As an important class of polymers of distinct branching architecture/topology and superior properties, star polymers containing multiple arms joined at a central core have received extensive research attention in the past decade. Like dendrimers and hyperbranched polymers, star polymers possess highly compact nanoscale three-dimensional globular structures with tunable inner and peripheral functionalities, which impart them many desired properties including high solubility, tremendously reduced melt and solvent viscosity, and the presence of a high degree of functional groups ready for further functionalization.[1,2] These remarkable structural and performance features have encouraged their emerging applications in various areas including drug delivery,[3] coating,[4] rheology modification,[5] bioimaging,[6] compartmented catalysis,[7] etc. Synthesis of star polymers, particularly those of well-defined arm length and number, is often achieved with the use of "living" or controlled polymerization techniques due to their significantly better control of polymer molecular weight development and polydispersity. The typical "living" polymerization techniques employed in the synthesis include the classical "living" anionic[2b,8] and cationic polymerizations,[9] "living" ring-opening polymerization,[10] "living" ring-opening metathesis polymerization,[11] and "living" or controlled radical polymerization.[12−16] In particular, the recent developments of "living" or controlled radical polymerization techniques, including the most notable atom-transfer radical polymerization (ATRP), have expanded tremendously the scope and flexibility in the synthesis of star polymers, with a large class of well-defined star polymers successfully synthesized from various monomer stocks.[12−16]

With "living" polymerization techniques as the tool, three major synthetic strategies—"arm-first", "core-first", and "coupling-onto"—have been commonly employed in synthesis of star polymers. The "arm-first" strategy involves the first preparation of "living" polymer arms or macroinitiators (MIs) capable of further chain extension and their subsequent end-joining by

Received: February 20, 2011
Revised: April 23, 2011
Published: May 09, 2011

ACS Publications © 2011 American Chemical Society

initiating polymerization of cross-linkable monomers, such as divinyl monomers. Star polymers synthesized with the "arm-first" strategy are generally featured with a highly cross-linked core containing abundant reactive groups, which may potentially be employed for further encapsulation of valuable guest species such as catalytic metal centers for other desired reactions.[12g] Meanwhile, this strategy also has the advantage of precisely controlling the arm length, and enabling synthesis of miktoarm star polymers containing arms of mixed sizes or chemical identities via either the "in−out" or mixed MI approaches.[1,2] With "arm-first" strategy in combination with the ATRP technique, Matyjaszewski et al.,[13] Sawamoto et al.,[14] and Chen et al.[15] have respectively synthesized successfully a variety of star polymers from different monomer stocks, such as styrenics, methacrylates, and acrylates. In the "coupling-onto" strategy, preformed polymer arms bearing an end functional group are reacted with a multifunctional core molecule containing complementary reactive groups. Highly efficient coupling reactions, like the "click reaction", are often required in order to achieve high coupling efficiency and to synthesize star polymers of well-defined arm numbers.[16] Differently, the "core-first" strategy requires specifically the use of specially designed multifunctional initiators, which can be used to initiate simultaneous multidirectional "living" growth of polymer arms from multiple initiating sites bound on the central core. Compared to the other two, the "core-first" strategy has the advantage of offering a more precise control over arm number by tailoring the number of functionalities of the multifunctional initiators.[1,8−12] A variety of multifunctional initiators have been successfully developed to suit each of the above "living" polymerization techniques for "core-first" synthesis of star polymers from different monomer stocks.

In sharp contrast to the great success achieved in star polymer synthesis with other types of "living"/controlled polymerization techniques, synthesis of star polyolefins from olefin monomer stocks (like ethylene and propylene) by using the "living" olefin coordination polymerization technique has lagged behind tremendously.[17] Though this "living" polymerization technique has advanced significantly in the past decades with the discovery of a great number of well-behaved transition metal catalysts,[18] it has rarely been developed/employed for synthesis of star polyolefins except few but important breakthroughs achieved very recently. To this end, our research group demonstrated the first synthesis of three-arm symmetrical star polyethylenes (PEs) through the "core-first" ethylene "living" polymerization with a trinuclear Pd−diimine catalyst.[17a] Very recently, we further reported the "core-first" synthesis of multiarm star PEs bearing a hyperbranched PE core and multiple (ca. 20−27 per star) linear-but-branched PE arms through ethylene multifunctional "living" polymerization with multinuclear Pd−diimine catalysts bound on a hyperbranched PE core.[17b] These star PEs have been confirmed to have well-defined narrow-distributed arm length and well-controlled arm number or average arm number. The unique synthetic and polymerization chemistry of Pd−diimine complexes enabled our successful design of these novel multinuclear Pd catalysts that can unprecedentedly initiate and catalyze simultaneous three- or multidirectional "living" chain growth from a common core.[17,19] In addition to our reports, Dong et al. reported recently the synthesis of three-arm star isotactic polypropylenes by "click" coupling functionalized isotactic polypropylene chains containing an end azide group with a trialkyne core.[20] The resulting star polymers in their report are featured with a broad arm length distribution due to the nonliving nature of the metallocene-catalyzed propylene polymerization adopted for arm synthesis.

In an effort to further broaden the scope and flexibility in synthesis of star polyolefins with "living" polymerization techniques, we demonstrate in this paper the first example of "arm-first" synthesis of star PEs through a two-step tandem polymerization process combining the ethylene "living" polymerization technique with ATRP of divinylbenzene (DVB) (Scheme 1). In the first step, coordinative ethylene "living" polymerization is undertaken to synthesize well-defined PE MIs containing a 2-bromoisobutyryl end group active for initiating ATRP with a uniquely functionalized Pd−diimine catalyst, $[(ArN{=}C(Me){-}(Me)C{=}NAr)Pd(CH_2)_3C(O)O(CH_2)_2OC(O)C(CH_3)_2{-}Br]^+SbF_6^-$ (Ar = 2,6-$(iPr)_2C_6H_3$) (**1** in Scheme 1), as we demonstrated in our previous work.[21] Serving as the polymer arms, these narrow-distributed PE MIs are subsequently used to initiate ATRP of cross-linkable DVB in the second step to render star polymers having a cross-linked core. Aiming at obtaining star polymers having well-defined arm length and controllable average arm number, a systematic study is undertaken to investigate the effects of various polymerization parameters in the ATRP step on the star formation process and the structural parameters of the resulting star polymers. Meanwhile, dilute solution properties of this novel range of star PEs are also characterized to establish their correlations with the arm length and number, and to disclose their highly compact chain conformation.

EXPERIMENTAL SECTION

Materials. All manipulations involving air- and/or moisture-sensitive compounds were carried out in a N_2-filled glovebox or using Schlenk techniques. The functionalized Pd−diimine catalyst **1**, $[(ArN{=}C(Me){-}(Me){-}C{=}NAr)Pd(CH_2)_3C(O)O(CH_2)_2OC(O){-}C(CH_3)_2Br]^+SbF_6^-$ (Ar = 2,6-$(i\mathrm{Pr})_2C_6H_3$), was synthesized according to our previous paper.[21] Ultrahigh-purity N_2 (>99.97%) and polymer-grade ethylene (both from Praxair) were purified by passing through 3 Å/5 Å molecular sieves and Oxiclear columns to remove moisture and oxygen, respectively, before use. HPLC-grade chlorobenzene (99.5%, Aldrich) and toluene (99.5%, Fisher Scientific) were deoxygenated and dried by using a commercial solvent purification system (Innovative Technology) before use. CuBr (99.999%, Aldrich) was purified before use by stirring in glacial acetic acid, followed with washing with methanol and drying under vacuum. DVB (80%, mixture of isomers) was distilled under vacuum to remove the inhibitor before use. Other chemicals, including $CuBr_2$ (>99%, Aldrich), *N*,*N*,*N*′,*N*″,*N*″-pentamethyldiethylenetriamine (PMDETA, 99%, Aldrich), anhydrous dichloromethane (99.8%, Aldrich), anhydrous diethyl ether (>99%, Aldrich), tetrahydrofuran (THF, ACS reagent grade, Fisher Scientific), and methanol (ACS reagent, Fisher Scientific) were all used as received.

Synthesis of PE MIs by Ethylene "Living" Polymerization with 1. The following is the typical ethylene "living" polymerization procedure used for synthesis of macroinitiator MI1 listed in Table 1. It is similar to those used in our previous works with various Pd−diimine catalysts.[17,21,22] The polymerization was carried out at 400 psi and 5 °C in a 500 mL Autoclave Engineers Zipperclave reactor equipped with a MagneDrive agitator and a removable heating/cooling jacket. The reactor temperature was maintained by passing a water/ethylene glycol mixture through the jacket using a refrigerating/heating circulator set at the desired temperature. The reactor was cleaned carefully with toluene and acetone, followed with an vacuum/nitrogen purge procedure at 70 °C for three cycles, and was then cooled down to 5 °C under nitrogen protection. Under nitrogen protection, chlorobenzene (50 mL) and freshly prepared catalyst **1** solution in chlorobenzene (20 mL, containing

Scheme 1. Two-Step "Arm-First" Synthesis of Polyethylene Star Polymers with a Cross-Linked Core by Combining Pd-Catalyzed Ethylene "Living" Polymerization with ATRP of Divinylbenzene

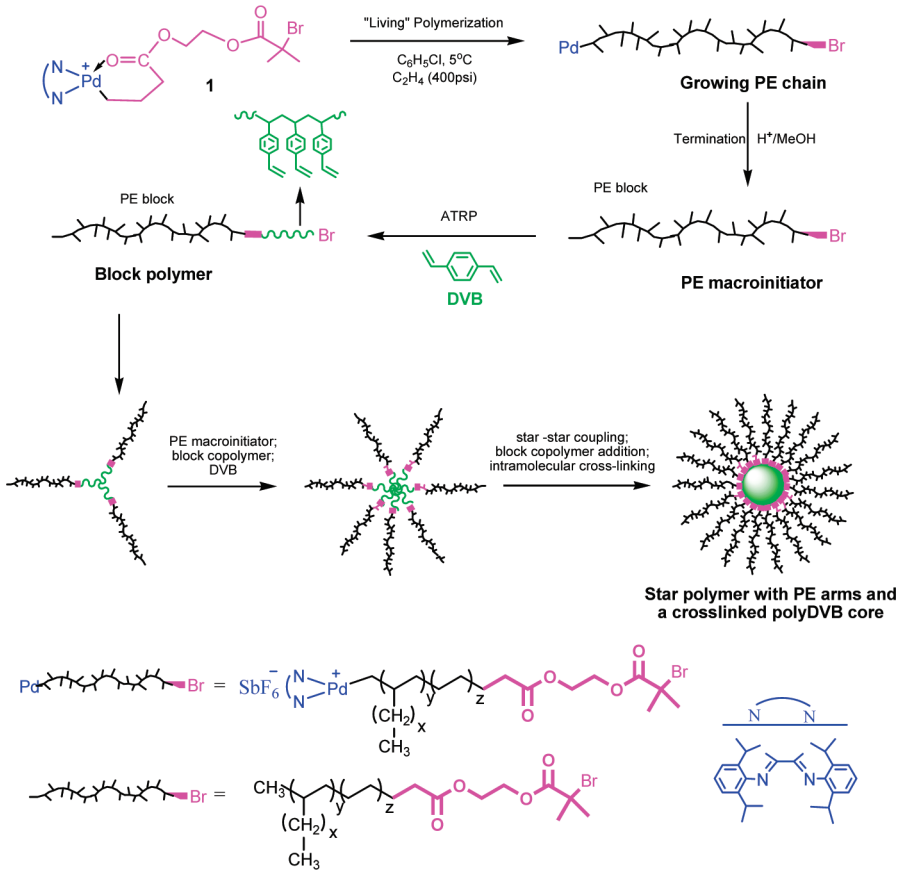

Table 1. Synthesis of Three PE MIs with Different Lengths via Ethylene "Living" Polymerization with Catalyst 1[a]

MI	time (h)	TOF[b](1/h)	$M_{n,LS}$[c](kg/mol)	$M_{w,LS}$[c](kg/mol)	PDI_{LS}[c]	$M_{n,NMR}$[d](kg/mol)	branching density[e](/1000 C)	$[\eta]_w$[f](mL/g)
MI1	1	173	7.3	7.4	1.01	7.1	88	14.4
MI2	1.5	190	10.3	10.4	1.01	10.3	87	18.2
MI3	2	214	13.7	13.9	1.02	13.6	86	20.6

[a] Other conditions: catalyst **1** amount, 0.3 mmol for MI1, 0.2 mmol for MI2, and 0.15 mmol for MI3; solvent, chlorobenzene; total volume, 70 mL; ethylene pressure, 400 psi; temperature, 5 °C. [b] Ethylene turnover frequency (TOF) determined gravimetrically on the basis of moles of catalyst employed and the mass of polymer produced. [c] Absolute number-average molecular weight ($M_{n,LS}$), weight-average molecular weight ($M_{w,LS}$), and polydispersity index (PDI_{LS}) data were determined with the light scattering detector in triple-detection GPC measurements. [d] Number-average molecular weight ($M_{n,NMR}$) data were determined with ^{1}H NMR spectroscopy based on end group analysis. [e] Branching density data were determined with ^{1}H NMR spectroscopy. [f] Weight-average intrinsic viscosity ($[\eta]_w$) data were determined with the viscosity detector in triple-detection GPC measurements.

0.3 mmol catalyst) were injected into the reactor. The solution was stirred for ca. 10 min to establish the equilibrium temperature at 5 °C. After releasing the nitrogen pressure, the reactor was then quickly pressurized to an ethylene pressure of 400 psi to start the polymerization. During the polymerization, ethylene pressure was maintained at 400 psi and the temperature was controlled at 5 °C by using the circulator. After 1 h, ethylene pressure was released, the polymer solution was collected and poured into a large amount of 2%-acidified methanol to precipitate out the polymer product. The polymer precipitate was redissolved in THF. The solution was then filtered with a 0.2 μm Teflon syringe filter to remove Pd particles, followed with precipitation in methanol. This dissolution−precipitation procedure was repeated until the polymer product was clear. After drying under vacuum at 50 °C for 2 days, 1.45 g of MI1 was obtained.

Synthesis of Star Polymers via ATRP of DVB with PE MIs.

Representatively, the following is an ATRP procedure for run 6 listed in Table 3. The PE MI (MI1, 0.150 g, 0.0211 mmol), toluene (4.58 g, ca. 5.2 mL), divinylbenzene (0.417 g, 2.56 mmol, 120 equiv), and PMDETA (49.5 mg, 0.283 mmol, 13.2 equiv) were added into a 20 mL glass tube used as the reactor. The reactor was sealed with a rubber septum and the mixture was stirred with a magnetic stirrer. After the complete dissolution of the PE MI in toluene, the mixture was subject to three freeze−pump−thaw cycles and was finally filled with nitrogen. CuBr (37.1 mg, 0.256 mmol) and $CuBr_2$ (5.61 mg, 0.0249 mmol) were then added under nitrogen protection. After being stirred for 20 min under N_2 at room temperature, the reactor was placed in a thermostated oil bath set at 95 °C to start the polymerization. Throughout the polymerization, the reaction system was protected by dry nitrogen. Samples

dx.doi.org/10.1021/ma2003954 |*Macromolecules* 2011, 44, 4125–4139

were taken at 1, 3, 6, and 22 h during the polymerization to monitor DVB conversion with gas chromatography and the molecular weight of the evolving star polymers with gel permeation chromatography. For each polymerization solution sampled from the reactor, the polymer was obtained by precipitating the majority of the polymerization mixture in methanol, followed with further wash with a large amount of methanol for three times and subsequent drying overnight under vacuum at room temperature.

To determine DVB conversion during ATRP, a small but precise volume of each polymerization solution taken from the reactor at different polymerization times was precipitated in methanol containing 600 ppm anisole as internal standard, and was subsequently filtered with a 0.2 μm syringe filter to remove polymer. The filtered solution was subsequently analyzed with gas chromatography to determine the concentration of residual unreacted DVB, which was then used to calculate DVB conversion.

Characterizations and Measurements. Proton nuclear magnetic resonance (^{1}H NMR) spectra of the polymers were all obtained on a Varian Gemini 2000 spectrometer (200 MHz) at ambient temperature with CD_2Cl_2 or $CDCl_3$ as solvent. Gas chromatography (GC) analyses were carried out on a Varian CP3800 gas chromatograph system, which was equipped with a Varian 1177 injector, an FID detector, and a Rtx-5 low-polarity fused silica column (30 m × 0.32 (i.d.) × 0.25 μm film thickness, Restek). Ultrapure He and N_2 were used as the carrier gas. The injector and detector temperatures were 200 and 300 °C, respectively. The following oven temperature program was used for the analysis: 60 °C for 1 min, followed with a ramp from 60 to 80 at 2.5 °C/min and, subsequently, from 80 to 280 at 50 °C/min.

Polymer characterizations with triple-detection gel permeation chromatography (GPC) were carried out on a Polymer Laboratories PL-GPC220 system equipped with a triple-detection array comprising of a differential refractive index (DRI) detector (from Polymer Laboratories), a three-angle (45, 90, and 135°) light scattering (LS) detector (from Wyatt Technology) at a laser wavelength of 687 nm, and a four-bridge capillary viscosity detector (from Polymer Laboratories). One guard column (PL# 1110−1120) and three 30 cm columns (PLgel 10 μm MIXED-B 300 × 7.5 mm) were used for polymer fractionation. This triple-detection GPC technique has been used extensively in our earlier works.[17,22c,23] HPLC-grade THF was used as the mobile phase at a flow rate of 1.0 mL/min. The whole GPC system, including columns and detectors, was maintained at 33 °C. Polymers solutions with a concentration between 1.5 and 6.0 mg/mL were injected into the columns at an injection volume of 200 μL. Astra software from Wyatt Technology was used to collect and analyze the data from all three detectors. Two polystyrene narrow standards (from Pressure Chemicals) with a weight-average molecular weight (M_w) of 30 and 200 kg/mol, respectively, were used for the normalization of LS signals from three detecting angles, and for the determination of interdetector delay volume and band broadening, respectively. The DRI increment (dn/dc) value of 0.078 mL/g was used for all PE MIs, and the value of 0.185 mL/g was used for polystyrene standards.[17,22c,23] For each star polymer product, an average dn/dc value was calculated from the feed mass of PE MI (W_{MI}), feed mass of DVB (W_{DVB}) and its conversion (x) according to the following equation:

$$dn/dc_{avg} = dn/dc_{PE} \times \frac{W_{MI}}{W_{MI} + xW_{DVB}} + dn/dc_{polyDVB} \times \frac{xW_{DVB}}{W_{MI} + xW_{DVB}} \quad (1)$$

in which dn/dc_{PE} = 0.078 mL/g and $dn/dc_{polyDVB}$ = 0.185 mL/g.

Differential scanning calorimetry (DSC) measurements were performed on a TA Instrument Q100 DSC equipped with a refrigerated cooling system (RCS) under a N_2 atmosphere. The instrument was operated in the standard DSC mode and was calibrated with an indium standard. A N_2 purging flow of 50 mL/min was used. Samples (about 5 mg) were heated from room temperature to 160 °C at 10 °C/min and then cooled to −90 °C at 10 °C/min, the data were then collected in the second heating ramp from −90 to +160 °C at a 10 °C/min. Glass transition temperatures (T_g) were read as the middle of the change in heat capacity and the melting temperatures (T_m) were read as the maximum of the endothermic peaks.

RESULTS AND DISCUSSION

Synthesis of PE MIs with Different Chain Lengths by Ethylene "Living" Polymerization with Pd−Diimine Catalyst 1. Ethylene "living" polymerization with the functionalized Pd−diimine catalyst **1** was first conducted at an ethylene pressure of 400 psi and 5 °C to directly synthesize PE MIs containing an end-capping 2-bromoisobutyryl functionality. In the polymerization, catalyst **1** initiates and catalyzes the "living" polymerization from the Pd−CH_2 initiating site, rendering "living" chains containing the valuable 2-bromoisobutyryl functionality at the starting end. This efficient synthesis, along with the unique design of catalyst **1**, has been demonstrated in our previous paper and PE MIs synthesized using this method have been used successfully to prepare functionalized PE diblock polymers through chain extension via ATRP.[21] Herein, PE MIs are employed as the polymer arms to construct star polymers. Three PE MIs (MI1−MI3 in Table 1) having different chain lengths were synthesized by using different polymerization times (1, 1.5, and 2 h, respectively), in an attempt to subsequently obtain star polymers having different arm lengths in the next step. These polymers were characterized with ^{1}H NMR and triple-detection GPC incorporating DRI, LS, and viscosity detectors to elucidate their chain structures and molecular weight information, respectively.

Table 1 summarizes the polymerization and polymer characterization results. From triple-detection GPC, these MIs have the desired well-defined molecular weights, with absolute number-average molecular weight ($M_{n,LS}$, determined with LS detector) of 7.3, 10.3, and 13.7 kg/mol, respectively, and a low polydispersity index (PDI_{LS}) about 1.01 for all of them. Figure S1 in the Supporting Information shows the GPC elution traces of the three polymers. Their increasing molecular weight over time and low PDI data are the solid evidence confirming the "living" nature of the polymerization.[21] Figure S2 in the Supporting Information shows the ^{1}H NMR spectra of the three PE MIs. While the dominant signals arise from the methyl, methylene and methine protons of the ethylene sequences, the presence of the intact 2-bromoisobutyryl end group is verified on the basis of the minor but characteristic resonance signals a−d shown in the spectra. Assuming each chain contains one 2-bromoisobutyryl group, the number-average molecular weight ($M_{n,NMR}$) was also calculated from the NMR spectra by integrating the peaks for the ethylene sequences and the end group. The calculated data are also listed in Table 1 and are nearly identical to the corresponding $M_{n,LS}$ data determined separately with GPC for all three polymers. This good agreement verifies inversely the presence of one 2-bromoisobutyryl end group per polymer chain in all three polymers.

Characteristic of Pd−diimine PEs, the three polymers are highly branched with a branching density of ca. 87 branches per 1000 carbons (listed in Table 1) as calculated from the resonance signals of the ethylene sequences in their ^{1}H NMR spectra. Such

a branching structure is a result of the well-known inherent chain walking mechanism of the Pd−diimine catalysts in ethylene polymerization.[24] On the basis of our prior studies,[17,21,22,25] these polymers should still possess a linear chain topology containing primarily short branching structures despite the high branching density, as the catalyst chain walking distance is relatively short at the given polymerization condition (i.e., high ethylene pressure of 400 psi and low temperature of 5 °C). The distribution of short branch structures from methyl to hexyl and longer has been illustrated in our previous paper[21] and is not included herein.

Synthesis of Star Polymers by ATRP of DVB with PE MIs. ATRP of DVB was subsequently undertaken with the above-synthesized PE MIs to render star polymers containing a cross-linked polyDVB core and PE arms of different lengths and average numbers. DVB was chosen herein because of its high affinity to radical addition and a low self-propagation rate, which favor star formation under ATRP conditions compared to dimethacrylate and diacrylate cross-linkers.[13a] Following our previous optimization of ATRP conditions for synthesis of diblock polymers with these PE MIs,[21] we adopted to use low MI feed concentrations ($[MI]_0$), a high ratio of $[Cu^+]_0/[MI]_0$ = 12, and the initial addition of Cu^{2+} (10% of Cu^+) as deactivator in the ATRP system to suppress radical concentration, reduce radical coupling, and consequentially enhance initiation efficiency. For all ATRP runs, $CuBr/CuBr_2$/PMDETA was used as the catalyst system with toluene as solvent at 95 °C. With their highly branched structures shown above, all PE MIs are amorphous and are soluble in toluene even at room temperature.

As the common mechanism for a typical "arm-first" synthetic strategy, the star formation herein should start with the chain extension on the PE MI to form diblock polymers having a short polyDVB block, which contains pendant vinyl groups. Subsequent intermolecular reactions between the chain-end radicals and the pendant vinyl groups render star polymers having a cross-linked core joining PE arms with the arm number following a statistical distribution. Concomitantly, star−star coupling occurs generally through radical-pendant vinyl group reactions between two star molecules, further increasing the molecular weight and broadening molecular weight distribution.[2c] Typically, polymerization parameters, including MI concentration, amount of cross-linker, and MI length, affect tremendously the star formation process and the resulting star polymers.[2c,13−15] The effects of these parameters in this current system are investigated thoroughly with the aim of controlling arm length and average arm number in the resulting star polymers.

(1). Effect of the PE MI Concentration. Four ATRP runs (runs 1−4 in Table 2) with the use of the same macroinitiator MI1 were carried out at four different MI concentrations (1.9, 3.8, 5.9, and 7.8 mM, respectively) while at a fixed $[DVB]_0/[MI]_0$ ratio (termed subsequently as DVB ratio) of 45 to study the effect of MI concentration. This range of MI concentrations is generally lower compared to those (typically, 10−70 mM) commonly used in the literature while the DVB ratio is much higher (typically, 5−25 in the literature with higher ratios leading to gelation).[13−15] No gelation occurred in these runs within a total polymerization time of 22 h, despite the high DVB ratio employed, due to the use of lower MI concentrations herein. During the course of each run, aliquot samples were taken regularly (1, 3, 6, and 22 h) and were subsequently characterized with GC for determining DVB conversion and with triple-detection GPC for monitoring polymer molecular weight development. The polymerization and characterization results are all summarized in Table 2.

Figure 1 shows the kinetic plots of DVB conversion (x) versus polymerization time for the four runs. The semilogmarithmic plot of DVB conversion reveals approximately a first-order kinetics with reference to DVB within the first 6 h of polymerization, and the major DVB consumption occurs with this initial period in all these four runs. After 6 h, the DVB consumption is slowed down significantly in all the runs because of the encapsulation of the majority of the radicals within the cross-linked star cores, which leads to enhanced diffusion resistances for DVB to travel through the PE shell to react with those radicals. Comparing the four runs, increasing the MI concentration leads to a consistent and significant increase in fractional DVB conversion (e.g., from 0.26 in run 1 to 0.66 in run 4 at the same polymerization time of 22 h) due to the correspondingly enhanced radical concentration in the polymerization system.

Figure 2 shows the GPC elution traces recorded from the DRI detector in triple-detection GPC characterization for the four runs. Characteristic of star polymers by "arm-first" synthesis,[13−15] broad multimodal curves consisting of three overlapping peaks at evolving relative intensities are observed in all samples taken from the four runs. In each sample, the peak having the lowest molecular weight (i.e., highest elution volume) always has nearly identical elution volume as the macroinitiator, MI1, despite the different polymerization time in different runs. Its relative intensity is continuously reduced with the increase of polymerization time. On the basis of peak fitting, its peak elution volume has a small but continuous decrease with the increase of polymerization time in each run. Clearly, this peak should correspond to the unjoined linear PE-*b*-polyDVB block polymers containing a short slow-growing polyDVB block. The middle peak having a medium elution volume also has a nearly fixed peak elution volume in all the samples in each run, with decreasing relative intensity with the increase of polymerization time in each run. Moreover, its molecular weight is found to be always about twice of that for MI1 in all samples despite the different MI concentration and polymerization time, indicating that this peak should correspond to linear coupled polymers with two PE MIs coupled together through short polyDVB block(s). The third peak having the highest molecular weight (i.e., lowest elution volume) should be attributed to the desired star polymers. Different from the two linear polymer peaks, the star polymer peak moves continuously toward reduced elution volume while at increasing relative intensity as the polymerization progresses in each run. This indicates that both molecular weight (i.e., increasing arm number and core size) and yield of the star polymers increase with the progress of polymerization, at the consumption of the linear block and coupled polymers. With the increase of polymerization time, the star polymer peak quickly becomes the dominant one in each run, which is increasingly pronounced with the increase of MI concentration due to faster polymerization rates.

To determine quantitatively the yield of star polymers in each sample, deconvolution of the GPC elution curves were undertaken through peak fitting of the constituting three peaks by using a Gaussian function. In the fitting process, the linear block polymer peak and coupled polymer peak were assumed to have the same peak width and profile as the corresponding MI (shown in Figure S1, Supporting Information), though at different elution volumes. Successful fitting was achieved for all samples with this method. As a demonstration, Figure S3 in the Supporting

Table 2. Synthesis of Polyethylene Star Polymers with Cross-Linked Core via ATRP of DVB: Effect of MI Concentration on the Formation of Star Polymers [a]

						GPC results of overall polymer products[f]				GPC results of star polymers[h]						
run	$[MI]_0$[b] (mM)	time (h)	DVB convn[c] (%)	DVB content[d] (wt %)	dn/dc[e] (mL/g)	$M_{n,LS}$ (kg/mol)	$M_{w,LS}$ (kg/mol)	PDI_{LS}	star yield[g] (%)	$M_{n,LS}$ (kg/mol)	$M_{w,LS}$ (kg/mol)	PDI_{LS}	f_n[i]	$[\eta]_w$ (mL/g)	$R_{h,w}$ (nm)	α[j]
1	1.9	1	3.1	3.1	0.081	18.3	26.4	1.45	28	47.7	53.2	1.12	6.3	22.8	5.6	0.151
		3	8.3	7.9	0.086	25.1	38.2	1.52	43	58.2	65.9	1.13	7.3	20.0	5.8	0.066
		6	18	15	0.095	32.6	52.9	1.63	57	67.7	79.1	1.17	7.8	19.9	6.2	0.050
		22	26	21	0.101	48.6	88.7	1.83	66	104	125	1.20	11.2	18.2	7.0	0.003
2	3.8	1	13	13	0.091	22.4	33.5	1.49	40.	50.2	61.3	1.22	6.0	21.9	5.8	0.047
		3	24	20.	0.100	38.2	64.3	1.68	64	73.4	91.7	1.25	8.0	19.2	6.3	0.019
		6	32	25	0.105	59.9	112	1.88	71	118	152	1.28	12.1	17.3	7.2	−0.001
		22	48	34	0.114	123	214	1.75	75	216	276	1.27	19.5	16.9	8.8	0.015
3	5.9	1	11	10.	0.089	31.5	53.0	1.68	59	59.1	77.4	1.31	7.3	19.2	6.0	−0.035
		3	25	21	0.100	55.2	113	2.05	69	115	160.	1.39	12.5	16.9	7.2	−0.064
		6	37	28	0.108	96.7	192	1.96	71	197	263	1.33	19.3	16.6	8.5	−0.025
		22	51	35	0.115	234	395	1.68	72	404	518	1.29	35.9	16.5	10.7	0.016
4	7.8	1	21	18	0.098	47.5	87.1	1.84	67	96.3	122	1.27	10.8	18.7	6.9	−0.031
		3	39	29	0.109	122	203	1.66	74	210.	261	1.25	20.3	17.4	8.7	−0.041
		6	55	37	0.117	201	313	1.56	75	316	394	1.25	27.4	17.5	10.0	−0.009
		22	66	41	0.122	386	512	1.33	73	537	628	1.17	43.4	17.8	11.8	−0.014

[a] Polymerization conditions: macroinitiator, MI1 with a molecular weight ($M_{n,LS}$) of 7.3 kg/mol; $[MI1]_0$:[DVB]:$[CuBr]_0$:$[CuBr_2]_0$:$[PMDETA]_0$ = 1:45:12:1.2:13.2; solvent, toluene; temperature, 95 °C. [b] The initial concentration of macroinitiator MI1 in the polymerization. [c] DVB conversion determined with the use of gas chromatography. [d] The mass content of DVB in the overall polymer products, calculated from the feed mass of MI and the mass of consumed DVB. [e] Average refractive index increment of overall polymer products calculated according to eq 1. [f] Number-average molecular weight ($M_{n,LS}$), weight-average molecular weight ($M_{w,LS}$) and polydispersity index (PDI_{LS}) data of the overall polymer products at different time, measured with light scattering (LS) detector in triple-detection GPC measurements. [g] Star yield is the area percentage of star polymer to overall polymer product determined by fitting the GPC curves obtained from the DRI detector. [h] $M_{n,LS}$, $M_{w,LS}$ and PDI_{LS} data of the star polymers were determined by LS detector in triple-detection GPC, weight-average intrinsic viscosity ($[\eta]_w$) and weight-average hydrodynamic radius ($R_{h,w}$) of the star polymers were determined with the viscosity detector. In the calculation, the two lower-molecular-weight linear polymer peaks in each overall polymer product were excluded. [i] Number-average arm number (f_n) of star polymer calculated according to eq 2. [j] α is the Mark−Houwink exponent of the star polymers.

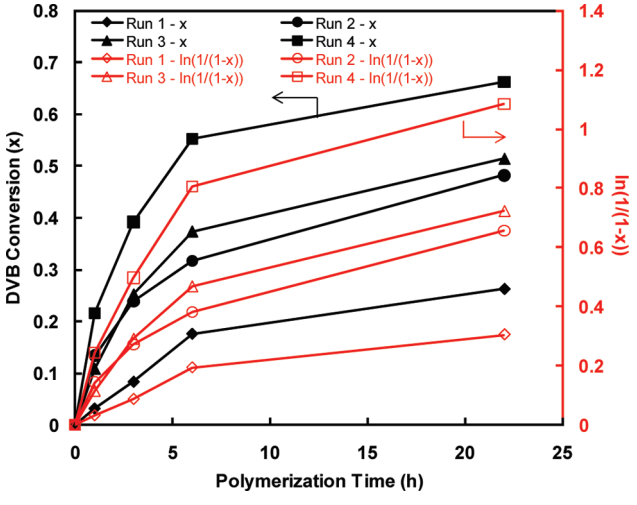

Figure 1. Kinetic plots of DVB conversion versus polymerization time in run 1 ($[MI1]_0$ = 1.9 mM), run 2 (3.8 mM), run 3 (5.9 mM), and run 4 (7.8 mM) at different MI concentrations. Other ATRP conditions: $[MI1]_0$:[DVB]$_0$:$[CuBr]_0$:$[CuBr_2]_0$:$[PMDETA]_0$ = 1:45:12:1.2:13.2, temperature = 95 °C, and toluene as solvent.

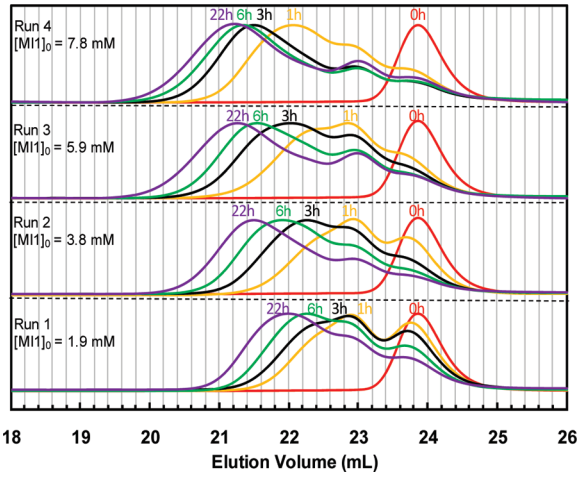

Figure 2. GPC elution traces (from DRI detector) of (a) run 1 ($[MI]_0$ = 1.9 mM), (b) run 2 (3.8 mM), (c) run 3 (5.9 mM), and (d) run 4 (7.8 mM).

Information shows the fitted curve and its constituting three peaks (with an overall fitting R^2 of 0.995) for the sample taken in run 2 at 22 h. The two linear polymer peaks have slightly reduced peak elution volumes (ca. 0.14 mL less) compared to the MI and the polymer having twice the molecular weight of the MI, respectively, which confirms the presence of short polyDVB

dx.doi.org/10.1021/ma2003954 |Macromolecules 2011, 44, 4125–4139

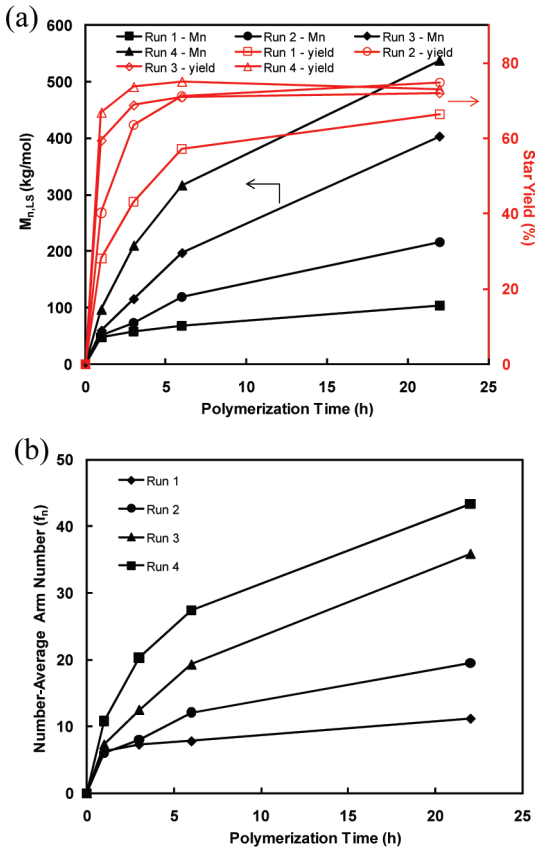

Figure 3. (a) Number-average molecular weight ($M_{n,LS}$) and yield of star polymers (with linear polymers excluded) and (b) number-average arm number (f_n) of the star polymers versus time in run 1 ($[MI1]_0$ = 1.9 mM), run 2 (3.8 mM), run 3 (5.9 mM), and run 4 (7.8 mM).

block(s) in these linear polymers. Subsequently, the area percentage of the star polymer peak relative to the area of the overall elution curve was calculated to give the yield of star polymers. These star polymer yield data are listed in Table 2 for all four runs and are also plotted in Figure 3a as a function of polymerization time.

With the LS detector of the triple-detection GPC, the absolute number- and weight-average molecular weights ($M_{n,LS}$ and $M_{W,LS}$) and polydispersity index (PDI_{LS}) data for both the overall polymer products (including linear and star polymers) and the star polymers (excluding linear polymers) were determined. In this determination of molecular weight with LS detection, the dn/dc value of the polymers is an important parameter. Herein, we adopt an average dn/dc value for all polymer portions in each overall polymer product, which is calculated according to eq 1 using the mass contents of both PE MI and DVB in the overall polymer product (calculated from MI feed mass and consumed DVB mass). It is assumed in this treatment that DVB is uniformly distributed through the whole molecular weight range in the overall polymer product. Given the presence of DVB block(s) in all three types of polymers (i.e., the linear block and coupled polymers, and star polymers), this treatment of the dn/dc value is justified. The calculated DVB content and dn/dc data are listed in Table 2 for all samples. In particular, the DVB content data reflect directly the size of the cross-linked DVB core in the star polymers.

For the overall polymer products, the molecular weight calculation was performed throughout the whole elution curve. For the star polymers, the calculation only includes the star polymer peak with the linear block and coupled polymers excluded. Figure S3 in the Supporting Information also shows an example of the selection of the star polymer peak for molecular weight calculation, whose low-molecular-weight portion overlapping with the linear polymers is truncated. This treatment may unavoidably lead to errors in the average molecular weights and meanwhile underestimates the polydispersity index of the star polymers, particularly in those lower-molecular-weight samples having significant peak overlapping between the star polymers and linear polymers. With the molecular weight data determined, the number-average arm number (f_n) in the star polymers is calculated according to

$$f_n = \frac{W_{MI}}{W_{MI} + xW_{DVB}} \times \frac{M_{n,star}}{M_{n,MI}} \quad (2)$$

where the first term in the calculation stands for the weight fraction of MIs in the star polymer with $M_{n,star}$ and $M_{n,MI}$ in the second term representing the number-average molecular weight of star polymers and MI, respectively. Even distribution of DVB in the overall polymer products is also assumed in this calculation. The molecular weight and arm number data are also summarized in Table 2. Figure 3 plots the dependencies of the yield, $M_{n,LS}$ and f_n of star polymers on polymerization time.

The yield of star polymers represents the conversion of the PE MIs into star polymers with high values desired. Herein, it shows positive dependencies on polymerization time and MI concentration. In each run, the yield increases quickly within the first few hours (6 h or less) to reach nearly a plateau value with only marginal changes afterward until the completion of the polymerization at 22 h (Figure 3a). For example, in run 3, the yield increases to the plateau value of 69% at 3 h which could be considered as the critical plateau point, with a minor change afterward to 72% at 22 h. It indicates that, at the critical plateau point, the majority of the star polymers formed should possess a highly congested shell, which makes the incorporation of additional linear polymers into the core difficult and subsequently leads to only minor changes in the yield afterward. From runs 1 to 4, the increase of MI concentration reduces the time needed to reach the critical plateau point due to the higher kinetic rate, while with only slight effect on final star yield at the completion of polymerization. For example, in contrast to run 3, the increase of star yield is much slower in run 1 given the lowest MI concentration, with 6 h needed to reach the yield of 57% followed with a further slow but continuous increase to 66% at 22 h without reaching a clear plateau.

The average molecular weights ($M_{n,LS}$ and $M_{W,LS}$) of the overall polymer products in each sample is significantly higher than that of MI1 due to star formation. They increase continuously with the increase of polymerization time in each run (see Table 2) even after reaching the critical plateau point due to the formation of more star polymers and/or star polymers of higher arm numbers and core sizes. In particular, the further significant increase of molecular weight after the critical plateau point indicates that star−star coupling is the dominant reaction contributing to molecular weight increase during this plateau region, as linear arms are rarely consumed in this period given the little change in star yield. From runs 1 to 4, increasing MI concentration improves dramatically the average molecular weights of the overall polymer products due to the enhanced concentration of

dx.doi.org/10.1021/ma2003954 |*Macromolecules* 2011, 44, 4125–4139

Table 3. Synthesis of Polyethylene Star Polymers with Cross-Linked Core via ATRP of DVB: Effect of DVB Ratio on the Formation of Star Polymers [a]

						GPC results of overall polymer products[f]				GPC results of star polymers[h]						
run	DVB ratio[b]	time (h)	DVB convn[c] s(%)	DVB content[d] (wt %)	d*n*/d*c*[e] (mL/g)	$M_{n,LS}$ (kg/mol)	$M_{w,LS}$ (kg/mol)	PDI_{LS}	star yield[g] (%)	$M_{n,LS}$ (kg/mol)	$M_{w,LS}$ (kg/mol)	PDI_{LS}	f_n[i]	$[\eta]_w$ (mL/g)	$R_{h,w}$ (nm)	α[j]
2	45	1	13	13	0.091	22.4	33.5	1.49	40.	50.2	61.3	1.22	6.0	21.9	5.8	0.047
		3	24	20.	0.100	38.2	64.3	1.68	64	73.4	91.7	1.25	8.0	19.2	6.3	0.019
		6	32	25	0.105	59.9	112	1.88	71	118	152	1.28	12.1	17.3	7.2	−0.001
		22	48	34	0.114	123	214	1.75	75	216	276	1.27	19.5	16.9	8.8	0.015
5	90	1	11	19	0.098	28.2	46.4	1.64	65	50.0	68.9	1.38	5.5	18.6	5.6	0.005
		3	22	31	0.111	57.8	102	1.76	74	98.3	133	1.34	9.3	16.5	6.8	0.040
		6	31	40.	0.121	125	220	1.76	78	197	273	1.39	16.3	15.9	8.5	0.051
		22	48	50.	0.132	381	539	1.41	81	487	624	1.28	33.3	16.1	11.3	0.109
6	120	1	16	31	0.111	30.5	45.9	1.51	70.	53.3	65.2	1.22	5.0	18.8	5.6	0.036
		3	30	45	0.126	73.8	129	1.75	77	121	162	1.34	9.1	16.6	7.3	0.076
		6	41	53	0.134	182	281	1.54	81	258	335	1.30	16.7	15.3	9.0	0.090
		22	51	58	0.141	593	754	1.27	85	666	832	1.25	37.7	16.6	12.7	0.170
7	180	1	6.8	22	0.102	59.4	104	1.74	75	104	141	1.35	11.1	14.0	6.5	0.088
		3	24	50.	0.131	205	329	1.61	82	293	391	1.33	20.1	14.9	9.4	0.120
		6	39	62	0.144	493	702	1.43	87	569	777	1.37	29.8	16.2	12.2	0.167
		22	gelled													

[a] Polymerization conditions: macroinitiator, MI1 with a molecular weight ($M_{n,LS}$) of 7.3 kg/mol; $[MI1]_0$ = 3.8 mM; $[MI1]_0$:$[CuBr]_0$:$[CuBr_2]_0$:$[PMDETA]_0$ = 1:12:1.2:13.2; solvent, toluene; temperature, 95 °C. [b] The initial concentration ratio of DVB to MI, $[DVB]_0/[MI]_0$. [c] DVB conversion was determined with the use of gas chromatography. [d] The mass content of DVB in the overall polymer products, calculated from the feed mass of MI and the mass of consumed DVB. [e] Average refractive index increment of overall polymer products calculated according to eq 1. [f] Number-average molecular weight ($M_{n,LS}$), weight-average molecular weight ($M_{w,LS}$), and polydispersity index (PDI_{LS}) data of the overall polymer products at different time, measured with light scattering (LS) detector in triple-detection GPC measurements. [g] Star yield is the area percentage of star polymer to overall polymer product determined by fitting the GPC curves obtained from the DRI detector. [h] $M_{n,LS}$, $M_{w,LS}$ and PDI_{LS} data of the star polymers were determined with LS detector in triple-detection GPC, weight-average intrinsic viscosity ($[\eta]_w$) and weight-average hydrodynamic radius ($R_{h,w}$) of the star polymers were determined with the viscosity detector. In the calculation, the two lower-molecular-weight linear polymer peaks in each overall polymer product were excluded. [i] Number-average arm number (f_n) of star polymer calculated according to eq 2. [j] α is the Mark−Houwink exponent of the star polymers.

star polymers, which enhances star−star coupling to render bigger stars of even higher molecular weights.

The molecular weight distribution of the overall polymer products is much broader compared to the narrow-distributed MI1, which is characteristic of "arm-first" star polymers.[13−15] For all the four runs, the PDI data of the overall polymer products show an interesting correlation to the star yield. As a common feature in each run, the PDI value increases with the increase of star yield until reaching the critical plateau point, after which the PDI value drops instead with further minor increase of star yield (see Table 2). For example, in run 3, the PDI values increases from 1.68 at star yield of 59% (1 h) to 2.05 at 69% (3 h, critical plateau point), and then drops to 1.96 at 71% (6 h) and to 1.68 at 72% (22 h). Differently, in run 1, the PDI value has a continuous increasing trend from 1.45 at yield of 28% (1 h) to 1.83 at 66% (22 h) as a plateau yield was not reached until probably the end in this run. In run 4, the PDI value decreases continuously from 1.84 at the yield of 67% (1 h) to 1.33 at 73% (22 h) since the critical plateau point is reached at ca. 1 h. This phenomenon is also found in the other runs to be reported in subsequent sections. It suggests that there is an increasingly broader size distribution of star polymers with the time increase before reaching the critical plateau point with the continuous consumption of MI and, afterward, statistical star−star coupling as the dominant reactions narrows autonomously the size distribution by favoring the coupling among smaller sized less sterically encumbered star polymers.

Compared to the corresponding overall polymer products, the star polymers have higher $M_{w,LS}$ and $M_{n,LS}$ data and reduced PDI_{LS} values as expected due to the exclusion of the lower-molecular-weight linear polymers. With the increase of polymerization time, the average molecular weights of the star polymers increase in each run with only small changes in their PDI values (generally between 1.10−1.39). From Figure 3b, the average arm number, f_n, increases with polymerization time and MI concentration, with the highest value of 43.4 reached in run 4 at 22 h.

(2). Effect of DVB Ratio. To investigate the effect of the amount of DVB on star formation, three additional runs (runs 5−7) were carried out under identical conditions as run 2 with MI1 at a concentration of 3.8 mM, with the exception of the DVB ratios (90, 120, and 180, respectively, as opposed to 45 for run 2). The selection of this low MI concentration for this investigation was on the basis of the relatively high star yield and slow star formation achieved at this condition as found above. Table 3 lists all the polymerization and polymer characterization results for these runs. Among these runs, gelation occurred only in run 7 after 6 h, which was performed at the highest DVB ratio of 180.

Figure 4 compares the kinetic plots of the four runs. As was observed in the study of the effect of PE MI concentration, the DVB consumption occurred primarily within the first 6 h by

dx.doi.org/10.1021/ma2003954 |*Macromolecules* 2011, 44, 4125–4139

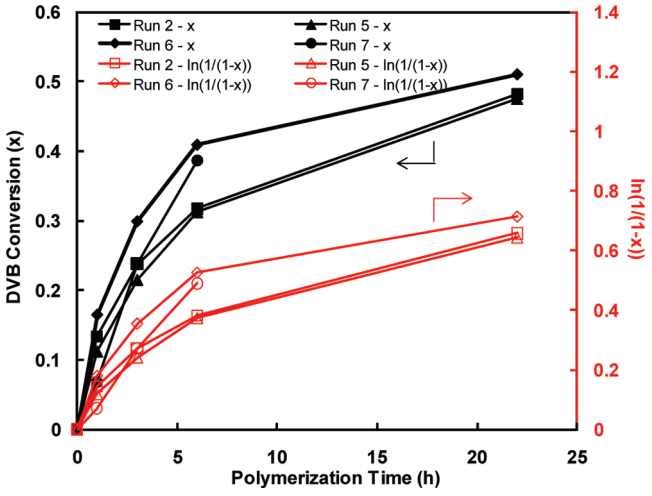

Figure 4. Kinetic plots of DVB conversion versus time in four runs at different DVB ratios, run 2 ($[DVB]_0/[MI]_0$ = 45), run 5 (90), run 6 (120), and run 7 (180) with MI1 at 3.8 mM. Other ATPR conditions: $[MI1]_0$:$[CuBr]_0$:$[CuBr_2]_0$:$[PMDETA]_0$ = 1:12:1.2:13.2, temperature = 95 °C, and toluene as solvent.

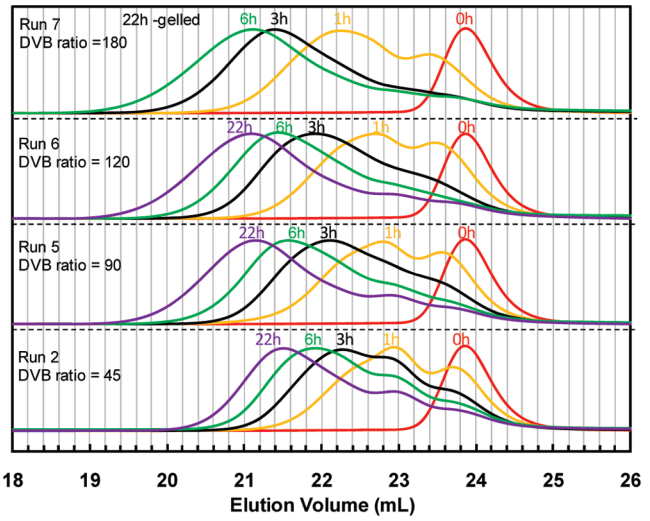

Figure 5. GPC elution traces (from DRI detector) of run 2 ($[DVB]_0/[MI1]_0$ = 45), run 5 (90), run 6 (120), and run 7 (180).

following approximately first-order kinetics. There is no distinct effect of the DVB ratio on the pattern of the kinetic curves. Given the increasingly high DVB ratios in runs 5−7, the overall polymer products in these runs generally have high DVB contents (>31 wt %) after 3 h of polymerization. For example, the 6 h sample in run 7 has a DVB content of 62 wt % in the overall polymer product, which is much greater than the typical values of 10−30 wt % found for "arm-first" star polymers reported in the literature.[13] The star polymers synthesized herein thus have a relatively large sized polyDVB core. With the increase of DVB ratio and/or polymerization time, the core size should further increase. In a literature "arm-first" synthesis of star polymers with a polystyrene MI (PSt−Br) at an initial concentration of 70 mM, gelation occurred at 2.8 h at a low DVB ratio of 20.[13a] The absence of gelation (except in run 7 after 6 h) despite high DVB ratios, while yielding star polymers having relatively large core sizes, is attributed to the low MI concentration used herein, which reduces radical concentration, and thus minimizes undesired gelation through fast coupling of large stars or chain transfer. With the extremely high DVB content in run 7, gelation could not be avoided at the late stage of polymerization in this run. Because of the presence of a large number of reactive double bonds in the core, these star polymers were found to be sensitive to temperature, and postsynthesis gelation could occur if being dried at elevated temperatures (e.g., 60 °C). Given this, all the polymer products synthesized herein were dried under vacuum at room temperature to avoid the postsynthesis gelation.

Figure 5 compares the GPC elution traces (from DRI detector) of the four runs at different DVB ratios. Like those in Figure 2 in the previous section, the GPC elution traces are broad, also consisting of three overlapping peaks assignable to the star polymers, linear coupled polymers, and linear block polymers, respectively. With the increase of DVB ratio from run 2 to run 7, the DVB block in the linear polymers appear to get longer, which can be verified from the slightly reduced elution volumes of both linear polymer peaks (e.g., by comparing the peak elution volumes for the 1 h samples in the four runs). Meanwhile, the rates at which the star polymer peak gains intensity and moves left toward reduced elution volume are also enhanced with the increase of DVB ratio from run 2 to run 7. Particularly, in run 7, the linear polymers nearly vanished after 3 h of polymerization with only weak peak intensities relative to the star polymer peak.

Using the same peak fitting and calculation methods demonstrated above, the star yield and molecular weight data for both overall polymer products and star polymers were determined. These data are summarized in Table 3 and Figure 6. From Figure 6a, the star yield generally reaches a plateau at about 6 h in each run, with little increase afterward. Increasing the DVB ratio in runs 2 to 7 leads to pronounced increases in the star yield. For example, the star yield at 6 h is 71, 78, 81, and 87, respectively, for runs 2−7. Consistent with literature reports,[13−15] high DVB ratios are thus necessary in order to increase star yield and minimize the presence of residual linear polymers in the overall polymer products. The $M_{n,LS}$ and f_n data of the star polymers depend sensitively on the DVB ratio at a given polymerization time, with both increasing sharply with the increase of DVB ratio.[13−15] Meanwhile, the rates at which $M_{n,LS}$ and f_n increase as a function of time are also enhanced significantly with the increase in the DVB ratio (Figure 6a,b). For example, at 22 h, the f_n value is nearly doubled from 19.5 in run 2 to 37.7 in run 6. While the PDI data of the star polymers do not change significantly in each run, those of the overall polymer products follow the interesting trend noted above, with an initial increase followed with a subsequent decrease once reaching the critical plateau point.

(3). Effect of MI Length. The MI length or arm length has a complicating effect on the star formation in "arm-first" synthesis. On one hand, Matyjaszewski et al. have found in CuBr/PMDETA catalyzed ATRP systems that longer arms led to loose star polymers with reduced star yield, arm number, and molecular weight due to enhanced steric hindrance in the star shell, which restricts the further incorporation of more arms into a star macromolecule and/or the occurrence of the star−star coupling.[13b,c] This effect was also noted in "arm-first" synthesis of star polymers by ionic polymerizations.[26,27] On the contrary, Sawamoto et al. found in their experiments with $RuCl_2(PPh_3)$-catalyzed ATRP systems that an increase in arm length resulted

dx.doi.org/10.1021/ma2003954 |*Macromolecules* 2011, 44, 4125–4139

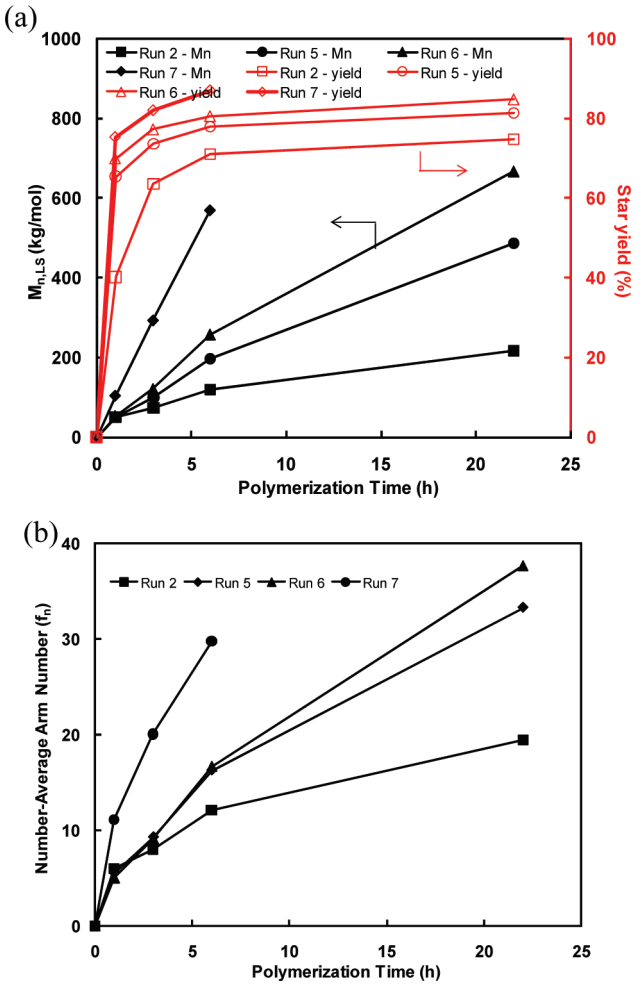

Figure 6. (a) Number-average molecular weight ($M_{n,LS}$) and yield of star polymers (with linear polymers excluded), and (b) number-average arm number (f_n) of the star polymers versus time in run 2 ($[DVB]_0/[MI1]_0 = 45$), run 5 (90), run 6 (120), and run 7 (180).

in increases in yield, arm number, and molecular weight of star polymers.[14b] These seemingly conflicting results were reasoned by Sawamoto et al. to stem from the different polymerization rates at different MI lengths in their polymerization system.[14b] Herein, the effect of arm length on star formation in this current system is investigated at a low MI concentration of 3.8 mM. In comparison with runs 5 and 7, three additional runs (runs 8−10) were carried out with the use of the other two MIs (MI2 and MI3, respectively). Among them, runs 8 and 9 were performed at the same DVB ratio of 90 as run 5, and run 10 was performed at the same DVB ratio of 180 as run 7. These two sets of experiments enable us to examine the effect of arm length under the two different conditions (i.e., different DVB ratios). Table 4 and Figures 7−9 summarize the polymerization results and polymer characterization data.

Parts a and b of Figure 7 compare the kinetic plots of the two sets of runs, respectively. For the set at the DVB ratio of 90, very similar kinetic curves are found for the three runs despite the different MI lengths (Figure 7a), indicating little effect of MI length on the polymerization kinetics under this condition. Comparing the other set (runs 7 and 10) at the DVB ratio of 180, the semilogarithmic kinetic curves for both runs are similar within the initial 3 h, after which the curve for run 10 with MI3 levels off significantly with a dramatically reduced DVB consumption rate. Moreover, no gelation occurred in run 10 throughout the polymerization (22 h) in contrast to the occurrence of gelation in run 7 after 6 h. These kinetic differences indicate that the steric hindrance resulting from the arm length does play at this condition of higher DVB ratio by slowing down DVB consumption rate and avoiding gelation.

Like the previous runs, similar evolutions of the GPC elution traces (see Figure S4 in Supporting Information) are observed in the three additional runs (runs 8−10). Parts a and b of Figure 8 demonstrate, respectively, the star yield, $M_{n,LS}$, and f_n data of the star polymers in the set of runs at the DVB ratio of 90. Increasing the arm length from MI1 (7.3 kg/mol) in run 5 to MI3 (13.7 kg/mol) in run 9 shifts down the star yield curves slightly but continuously, with negligible effect on the curve profile. For example, the final star yield at 22 h is 81, 78, and 75%, respectively, for runs 5, 8, and 9. The average arm number curves of the three runs are nearly identical (Figure 8b). Because of the increasing arm lengths at similar average arm numbers, the $M_{n,LS}$ data of the star polymers are enhanced correspondingly from run 5 to runs 8 and 9 at a given time (Figure 8a). The results from this set of runs reveal that the steric effect of arm length at this lower DVB ratio on the star formation is minor, with only marginal reduction in star yield. This insignificant effect may be attributed to two reasons: (1) the star formation at the given condition (i.e., low MI and DVB concentrations) is slow, with diffusion of macromolecules not being the limiting step; (2) the arm numbers of the star polymers are not high enough to generate significant steric effect at the given polymerization conditions.

Figures 9a,b compare the yield, $M_{n,LS}$ and f_n data for runs 7 and 10 at the DVB ratio of 180. Within the initial 3 h, the yield and f_n data of the two runs are very similar at a given time despite the different MIs, with $M_{n,LS}$ data being correspondingly greater in run 10 due to the longer arms. However, after 3 h, the yield and f_n data leveloff significantly in run 10. For example, at 6 h, the $M_{n,LS}$ and f_n values in run 10 are 516 kg/mol and 22.9, respectively, which are even lower than the corresponding values (569 kg/mol and 29.8, respectively) in run 7. Clearly, increasing arm length leads to reduced yield, $M_{n,LS}$, and f_n data in the late stage of polymerization at this condition. Compared to the previous set, the involvement of the steric effect in this set may be attributed to the higher arm numbers and/or faster star formation achieved herein at the higher DVB ratio of 180.

DSC Characterization. DSC characterization was performed selectively on the overall polymer products collected in run 5 to investigate the effect of star formation on thermal properties of the polymers. Figure 10 shows the DSC thermograms of the polymers obtained at different polymerization time, along with that of the corresponding macroinitiator MI1 for comparison. Characteristic of highly branched Pd−diimine polyethylenes, MI1 has a clear glass transition centered at ca. −65.3 °C and a weak broad melting endotherm in the temperature range from −60 to 10 °C with a peak temperature of ca. −28.3 °C.[17,21,22] In the overall polymer products, the glass transition and melting endotherm of the PE segments are continuously weakened, along with slight shifts to higher temperatures, with the progress of polymerization. In particular, in the 22 h sample, both transitions vanish. Apparently, the increasing steric crowdedness in the PE shell, resulting from the concomitant increases in arm number and core size of the star polymers during the polymerization, reduces the segmental mobility of the PE arms.[22b] In addition, a very

Table 4. Synthesis of Polyethylene Star Polymers with Cross-Linked Core via ATRP of DVB: Effect of MI Length on the Formation of Star Polymers[a]

							GPC results of overall polymer products[f]				GPC results of star polymers[h]						
run	MI	DVB ratio[b]	time (h)	DVB convn[c] (%)	DVB content[d] (wt %)	dn/dc[e] (mL/g)	$M_{n,LS}$ (kg/mol)	$M_{w,LS}$ (kg/mol)	PDI_{LS}	star yield[g] (%)	$M_{n,LS}$ (kg/mol)	$M_{w,LS}$ (kg/mol)	PDI_{LS}	f_n[i]	$[\eta]_w$ (mL/g)	$R_{h,w}$ (nm)	α[j]
5	MI1	90	1	11	19	0.098	28.2	46.4	1.64	65	50.0	68.9	1.38	5.5	18.6	5.6	0.005
			3	22	31	0.111	57.8	102	1.76	74	98.3	132	1.34	9.3	16.5	6.8	0.040
			6	31	40.	0.121	125	220	1.76	78	197	273	1.39	16.3	15.9	8.5	0.051
			22	48	50.	0.132	381	539	1.41	81	487	624	1.28	33.3	16.1	11.3	0.109
7	MI1	180	1	6.8	22	0.102	59.4	104	1.74	75	104	141	1.35	11.1	14.0	6.5	0.088
			3	24	50.	0.131	205	329	1.61	82	293	391	1.33	20.1	14.9	9.4	0.120
			6	39	62	0.144	493	702	1.43	87	569	777	1.37	29.8	16.2	12.2	0.167
			22	gelled													
8	MI2	90	1	11	14	0.093	42.5	75.4	1.78	65	85.2	111	1.31	6.9	23.6	7.2	0.016
			3	22	24	0.103	75.4	146	1.94	69	166	203	1.22	12.3	20.7	8.5	0.007
			6	33	32	0.113	148	273	1.84	76	277	351	1.27	18.2	20.2	10.1	0.017
			22	48	41	0.122	392	583	1.49	78	561	710	1.27	32.3	19.9	12.7	0.048
9	MI3	90	1	12	11	0.090	52.2	89.3	1.71	58	104	135	1.30	6.7	29.5	8.3	0.021
			3	25	21	0.100	112	208	1.86	67	226	288	1.28	13.0	26.5	10.3	−0.045
			6	35	27	0.107	140	263	1.88	71	283	358	1.26	15.1	25.2	10.9	−0.044
			22	50	34	0.115	522	737	1.41	75	740	905	1.22	35.4	24.4	14.8	−0.008
10	MI3	180	1	15	24	0.104	125	223	1.79	76	223	285	1.28	12.3	26.3	10.2	0.000
			3	26	36	0.116	317	407	1.28	80	408	474	1.16	19.1	24.5	12.0	−0.014
			6	31	39	0.120	421	513	1.22	77	516	598	1.16	22.9	23.8	12.9	−0.024
			22	34	42	0.123	572	698	1.22	75	691	805	1.17	29.2	23.3	14.0	−0.046

[a] Polymerization conditions: MI concentration, $[MI]_0$ = 3.8 mM; $[MI]_0$:$[CuBr]_0$:$[CuBr_2]_0$:$[PMDETA]_0$ = 1:12:1.2:13.2; solvent, toluene; temperature, 95 °C. [b] The initial concentration ratio of DVB to MI, $[DVB]_0/[MI]_0$. [c] DVB conversion was determined with the use of gas chromatography. [d] The mass content of DVB in the overall polymer products, calculated from the mass of MI and the mass of consumed DVB. [e] Average refractive index increment of overall polymer products calculated according to eq 1. [f] Number-average molecular weight ($M_{n,LS}$), weight-average molecular weight ($M_{w,LS}$) and polydispersity index (PDI_{LS}) data of the overall polymer products at different time, measured with light scattering (LS) detector in triple-detection GPC measurements. [g] Star yield is the area percentage of star polymer to overall polymer product determined by fitting the GPC curves obtained from the DRI detector. [h] $M_{n,LS}$, $M_{w,LS}$, and PDI_{LS} data of the star polymers were determined with LS detector in triple-detection GPC, weight-average intrinsic viscosity ($[\eta]_w$) and weight-average hydrodynamic radius ($R_{h,w}$) of the star polymers were determined with the viscosity detector. In the calculation, the two lower-molecular-weight peaks in each overall polymer product were excluded. [i] Number-average arm number (f_n) of star polymer calculated according to eq 2. [j] α is the Mark−Houwink exponent of the star polymers.

weak but observable transition at about 104 °C can also be found in the 1 h sample. In the other samples, such a weak transition can also be noticed though at different temperatures. Given the higher transition temperatures, this weak transition should result from polyDVB segments. As the cross-linked core has highly restricted mobility, this transition is attributed to the polyDVB blocks in the linear block and coupled polymers.

Dilute Solution Properties and Chain Conformation of Star Polymers. Dilute solution properties of these core-cross-linked star polymers, including the weight-average intrinsic viscosity ($[\eta]_w$), weight-average hydrodynamic radius ($R_{h,w}$), and Mark−Houwink exponent (α), were determined with the intrinsic viscosity detector, in conjunction with the LS detector, in triple-detection GPC characterization.[17] These data are also summarized in Tables 2−4. Determined on the basis of the angular dependency of light scattering, the R_g data for these star polymers could not be rigorously determined herein as they were found to be generally very small, below or only slightly above 10 nm (see the $R_{h,w}$ data for reference), which is the measurement limit in the multiangle LS technique.[28]

Parts a and b of Figure 11 demonstrate the Mark−Houwink plots of the star polymers (with linear polymers excluded) obtained at different polymerization times in five representative runs (runs 4 and 7 in Figure 11a; runs 5, 8, and 9 in Figure 11b). For the purpose of comparison, we have also included in the figures the intrinsic viscosity curve ($[\eta] = 0.0621M^{0.61}$ (mL/g)) constructed, in our earlier study, for linear polyethylenes synthesized with Pd−diimine catalysts having the same diiimine ligand as catalyst **1** at the same polymerization condition (400 psi and 5 °C).[17] As shown in the figures, the intrinsic viscosity values of the three MIs (MI1−MI3) are all well located on or very close to the curve, demonstrating they have the typical linear topology of polyethylenes synthesized at this condition.[17] These intrinsic viscosity plots enable us to investigate the separate effects of average arm number and arm length on the intrinsic viscosity and conformation of these star polymers. Specifically, the effect of average arm number can be revealed by comparing the intrinsic viscosity curves for the star polymers collected at different times in each run, given their increasing average arm number with the increase of polymerization time while at the fixed arm length. Meanwhile, the effect of arm length can be examined by

dx.doi.org/10.1021/ma2003954 |Macromolecules 2011, 44, 4125–4139

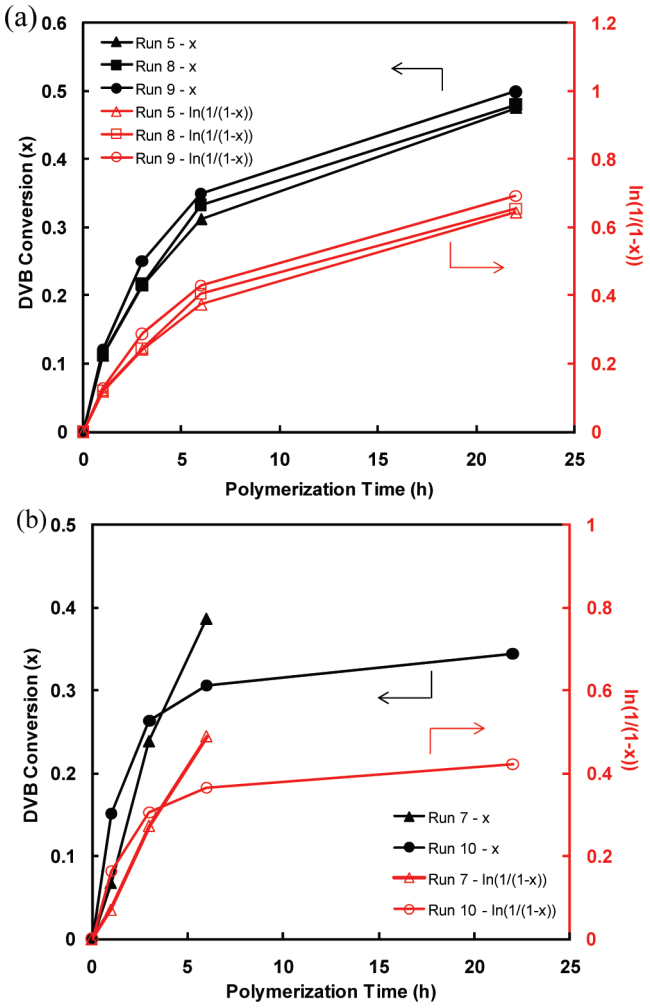

Figure 7. (a) Kinetic plots of DVB conversion versus time in run 5 (MI1 as arm), run 8 (MI2), and run 9 (MI3) at a DVB ratio 90 and $[MI]_0$ = 3.8 mM, and (b) kinetic plots of run 7 (MI1) and run 10 (MI3) at a DVB ratio of 180 and $[MI]_0$ = 3.8 mM. Other ATPR conditions: $[MI]_0$:$[CuBr]_0$:$[CuBr_2]_0$:$[PMDETA]_0$ = 1:12:1.2:13.2, temperature = 95 °C, and toluene as solvent.

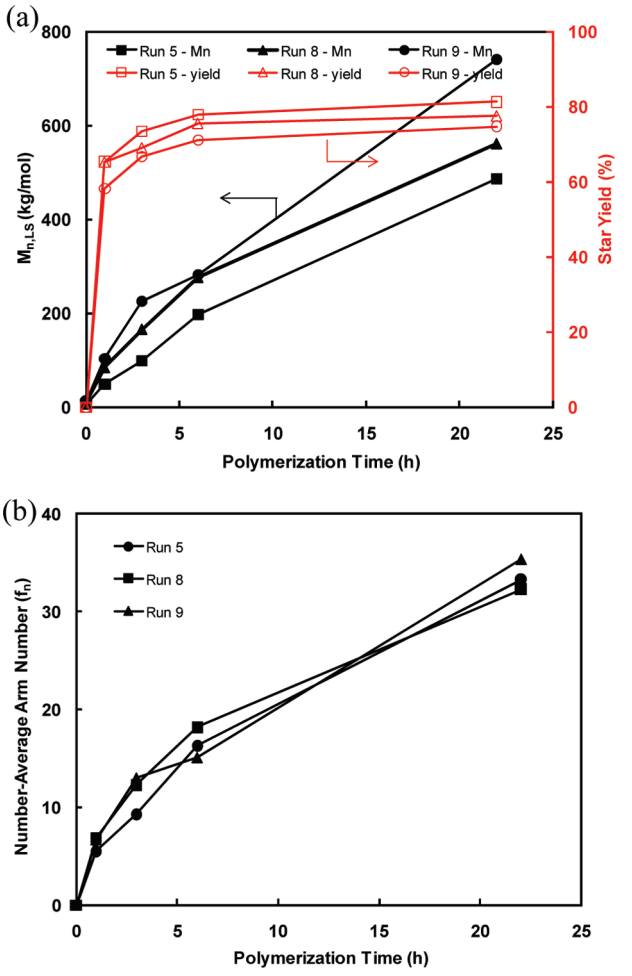

Figure 8. (a) Number-average molecular weight ($M_{n,LS}$) and yield of star polymers (with linear polymers excluded) and (b) number-average arm number (f_n) of the star polymers versus time in run 5 (MI1 as arm), run 8 (MI2), and run 9 (MI3) at a DVB ratio of 90.

comparing the curves for those synthesized with different MIs under the same conditions (those in runs 5, 8, and 9 in Figure 11b).

The α value is calculated as the slope of the intrinsic viscosity curve for each star polymer. Generally, all star polymers in all the runs have been found to have very weak dependencies of the intrinsic viscosity on molecular weight, generally with small positive α or even negative values in proximity to 0 (in the range of −0.05−0.1 as listed Tables 2−4), despite their very different arm lengths and average arm numbers. The value of α is sensitive to polymer chain conformation, typically with 0 for rigid spheres, 0.5 and 0.8 for flexible polymers in Θ solvents and good solvents, respectively, and 2 for rods.[28] Negative α values have been found with spherical dendrimers of high generations[29,30] and some star polymers of high arm numbers and molecular weights.[31] Some multiarm star polymers and hyperbranched polymers have also been demonstrated to behave as rigid spheres with zero α values, i.e., intrinsic viscosity does not change with molecular weight.[31−33] For "core-first" star polyethylenes containing multiple arms (about 20−27 arms per star) synthesized in our previous study,[17b] we have found the α values decrease interestingly from small positive numbers (ca. 0.20) to nearly zero and to even negative numbers (ca. −0.074) with the continuous increase of arm size from about 9.5 to 48 kg/mol, indicating their increasing resemblance to highly compact rigid spheres and high-generation dendrimers. Similarly, the low, nearly zero α values found herein for all star polymers demonstrate that these core-cross-linked star polymers also have highly compact chain conformation and behave like rigid spheres or high-generation dendrimers.[17b]

By examining all the runs, there is no general relationship found between the average arm numbers and α values. In each run, the α values vary slightly and do not have a clear trend of change with the increase of average arm number as the polymerization progresses. However, like our findings with the "core-first" star polyethylenes,[17b] the α values for these "arm-first" star polymers herein also decrease uniquely with the increase of arm length. Given their similar average arm numbers at any given polymerization time as illustrated above, the samples in runs 5, 8, and 9 well demonstrate this distinct relationship (Figure 11b). For example, the 6 h samples in runs 5, 8, and 9, which have very similar average arm numbers (16.3, 18.2, and 15.1, respectively), exhibit decreasing α values from 0.051 to 0.017 and to −0.044 with the increase of arm length from 7.3 kg/mol (run 5) to 10.3

dx.doi.org/10.1021/ma2003954 |*Macromolecules* 2011, 44, 4125–4139

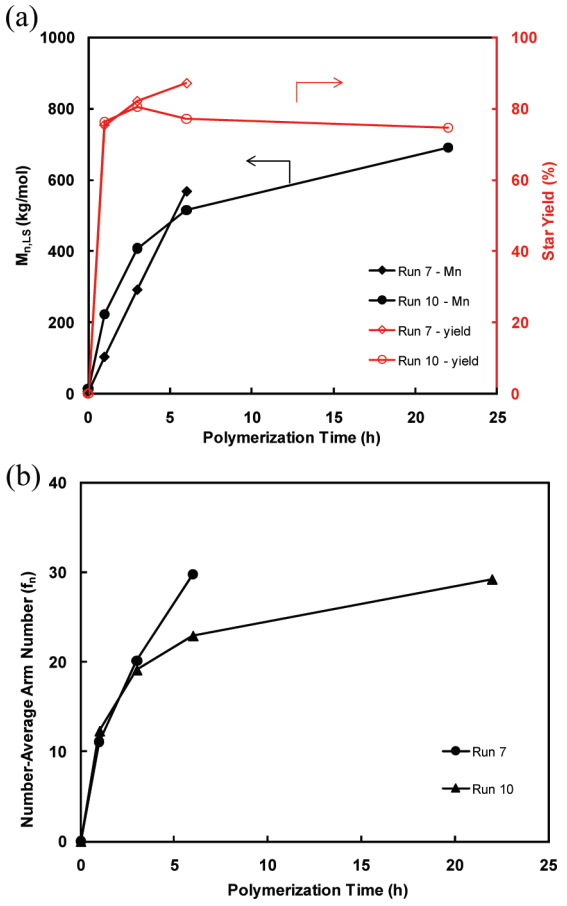

Figure 9. (a) Number-average molecular weight ($M_{n,LS}$) and yield of star polymers (with linear polymers excluded) and (b) number-average arm number (f_n) of the star polymers versus time in run 7 (MI1 as arm) and run 10 (MI3) at a DVB ratio of 180.

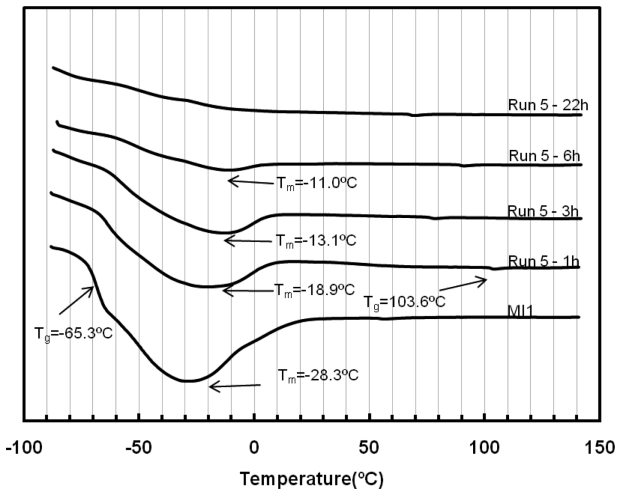

Figure 10. DSC thermograms of the overall polymer products collected in run 5 at different polymerization time.

kg/mol (run 8) and to 13.7 kg/mol (run 9). The same trend of change is also noted with the 3 and 6 h samples, respectively, in these three runs. Clearly, the increase of arm length renders star polymers with increasingly compact PE shells with more tightly

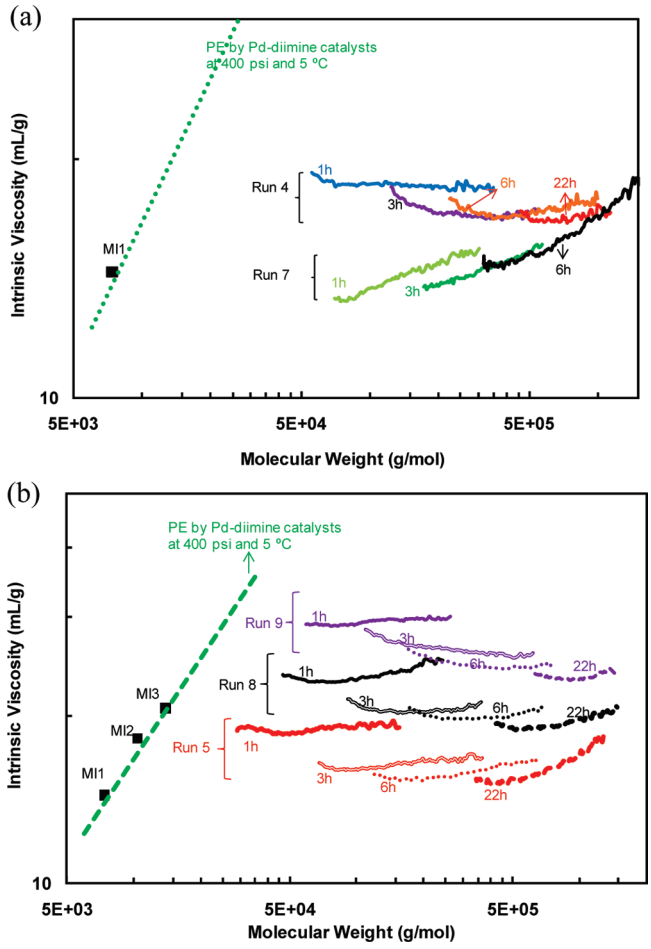

Figure 11. Mark–Houwink plots of star polymers (excluding the linear polymers) (a) in runs 4 and 7; and (b) in runs 5, 8, and 9. The intrinsic viscosity curve ($[\eta] = 0.0621\ M^{0.61}$ (mL/g)) for PE by Pd–diimine catalysts at 400 psi and 5 °C, included herein for comparison, was constructed in our earlier study.[17]

packed arms. Differently, the simultaneous increases of both average arm number and DVB core with the increase of polymerization time in each run do not appear to enhance compactness of the chain conformation.

Consistent with literature results on some multiarm star polymers[34] and our previous finding with "core-first" star PEs,[17b] the $[\eta]_w$ data of the star polymers synthesized herein are found to be affected primarily by the arm length, while not by the average arm number or by the polymer molecular weight. In each run, the star polymers collected at different polymerization times (3, 6, and 22 h) generally have very similar $[\eta]_w$ values with only little variations, indicating their independency of average arm numbers. This can also been seen from the nearly overlapping intrinsic viscosity curves shown in Figure 11 for the samples in each run. The exception is noted with the 1 h sample in each run, which always has the highest $[\eta]_w$ values compared to the other samples in the same run. This is believed to result from the significant contaminating presence of linear coupled and block polymers (particularly the coupled polymers) in these 1 h samples given their significant peak overlapping with star polymers at the initial polymerization period. All the star polymers synthesized with MI1 are found to have their $[\eta]_w$ data at about 16.5 mL/g regardless of the different runs at various conditions.

dx.doi.org/10.1021/ma2003954 |*Macromolecules* 2011, 44, 4125–4139

Similarly, those synthesized with MI2 and MI3 also have the similar $[\eta]_w$ data at about 20.5 and 24.0 mL/g, respectively. These $[\eta]_w$ data of the star polymers are much lower relative to the PE arms having equal molecular weights. Instead, compared to the $[\eta]_w$ data of the corresponding PE arms (14.4, 18.2, and 20.6 mL/g for MI1−MI3, respectively), the $[\eta]_w$ data of the star polymers herein, surprisingly, are only slightly (about 15%) greater. This differs from our finding with "core-first" multiarm star PEs synthesized in our previous study, which always have their $[\eta]_w$ data about twice the value of the constituting arms.[17b] Though the precise mechanism is unknown, this notable difference is hypothesized to result from their very different core sizes. Herein, these core-cross-linked "arm-first" star polymers have relatively large cores with high polyDVB core content up to 60 wt %, in sharp contrast to the relatively small cores (with content generally below 10 wt %) in the "core-first" star PEs synthesized in our previous study.[17b]

CONCLUSIONS

The "arm-first" synthesis of star PEs containing multiple linear-but-branched narrow-distributed PE arms and a cross-linked polyDVB core is demonstrated successfully in this work by using a two-step polymerization procedure combining ethylene "living" polymerization and ATRP of DVB. With the length and chain structure of the arms or MIs determined in the first ethylene "living" polymerization step, we have herein focused primarily on investigating the effects of various polymerization parameters (including MI concentration, DVB ratio, and MI length) in the ATRP step on the star formation kinetics, and on the arm number and molecular weight of the resulting star polymers. We have found that the low MI concentrations (1.9−7.8 mM) used herein are beneficial in avoiding the occurrence of gelation in the cross-linking polymerization of DVB while maintaining good star yield. Increasing the MI concentration leads to enhanced average arm number, star molecular weight, and a faster increase in star yield, but with little effect on final star yield. Increasing the DVB ratio helps increase the star yield and leads to star polymers with much higher average arm numbers and molecular weights. With the low MI concentrations used herein, we have found that the MI length generally has negligible steric effect on the polymerization kinetics, star yield, and average arm number of the star polymers, except in the late stage of polymerization when the highest DVB ratio (180) is used. By controlling these polymerization parameters along with polymerization time, a range of star PEs containing different arm lengths (7.3−13.7 kg/mol) and average arm numbers (ca. 5−43 per star) has been synthesized. DSC characterization of the thermal properties of the star polymers indicates that the segmental mobility of the PE arms is increasingly reduced with the increase of the average arm number. From the dilute solution properties determined with triple-detection GPC, the star polymers synthesized herein all have highly compact chain conformation and behave like rigid spheres and/or dendrimers with nearly zero α values. Their intrinsic viscosity has been found to depend only on the arm length, while with no dependency on average arm number or star molecular weight.

ASSOCIATED CONTENT

Supporting Information. GPC elution traces and ^{1}H NMR spectra of the three MIs, peak fitting of the GPC elution trace of a representative polymer product, GPC elution traces of runs 8−10, and ^{1}H NMR spectra of polymers synthesized in run 5. This material is available free of charge via the Internet at http://pubs.acs.org.

AUTHOR INFORMATION

Corresponding Author

*E-mail: zye@laurentian.ca (Z.Y.); wenjunwang@zju.edu.cn (W.J.W.).

ACKNOWLEDGMENT

The financial support from the Ontario Ministry of Research and Innovation as an Early Researcher Award (ERA) to Z.Y. is greatly appreciated. Z.Y. also thanks the Natural Science and Engineering Research Council (NSERC) of Canada, the Canadian Foundation for Innovation (CFI), and Canada Research Chair (CRC) program for funding research infrastructures. W.-J. W. and B.-G.L. thank the National Basic Research Program of China (973 Program 2011CB606001), the National Natural Science Foundation of China (Key Grant 20936006), the Program for Changjiang Scholars and Innovative Research Team in University in China, and the Chinese State Key Laboratory of Chemical Engineering at Zhejiang University (Grant No. SKL-ChE-11D02) for financial support. P.L. thanks the Hengyi Foundation at Zhejiang University for a scholarship for international student exchange.

REFERENCES

(1) Mishra, M.; Kobayashi, S., Eds. *Star and hyperbranched polymers*; Marcel Dekker Inc.: New York, 1999.

(2) Some review articles:(a) Inoue, K. *Prog. Polym. Sci.* **2000**, *25*, 453. (b) Hadjichristidis, N.; Pitsikalis, M.; Pispas, S.; Iatrou, H. *Chem. Rev.* **2001**, *101*, 3747. (c) Gao, H.; Matyjaszewski, K. *Prog. Polym. Sci.* **2009**, *34*, 317. (d) Blencowe, A.; Tan, J. F.; Goh, T. K.; Qiao, G. G. *Polymer* **2009**, *50*, 5.

(3) (a) Ooya, T.; Lee, J.; Park, K. *J. Controlled Release* **2003**, *93*, 121. (b) Wang, F.; Bronich, T. K.; Kabanov, A. V.; Rauh, R. D.; Roovers, J. *Bioconjugate Chem.* **2005**, *16*, 397.

(4) Groll, J.; Amirgoulova, E. V.; Ameringer, T.; Heyes, C. D.; Röcker, C.; Nienhaus, G. U.; Möller, M. *J. Am. Chem. Soc.* **2004**, *126*, 4234. (b) Lupitskyy, R.; Roiter, Y.; Tsitsilianis, C.; Minko, S. *Langmuir* **2005**, *21*, 8591.

(5) Wang, T. Y.; Tsiang, R. C.-C.; Liou, J.-S.; Wu, J.; Sheu, H.-C. *J. Appl. Polym. Sci.* **2001**, *79*, 1838.

(6) Fukukawa, K. I.; Rossin, R.; Hagooly, A.; Pressly, E. D.; Hunt, J. N.; Messmore, B. W.; Wooley, K. L.; Welch, M. J.; Hawker, C. J. *Biomacromolecules* **2008**, *9*, 1329.

(7) (a) Helms, B.; Guillaudeu, S. J.; Xie, Y.; McMurdo, M.; Hawker, C. J.; Fréchet, J. M. J. *Angew. Chem., Int. Ed.* **2005**, *44*, 6384. (b) Chi, Y.; Scroggins, S. T.; Fréchet, J. M. J. *J. Am. Chem. Soc.* **2008**, *130*, 6322. (c) Kanaoka, S.; Yagi, N.; Fukuyama, Y.; Aoshima, S.; Tsunoyama, H.; Tsukuda, T.; Sakurai, H. *J. Am. Chem. Soc.* **2007**, *129*, 12060.

(8) Some examples:(a) Lee, J. S.; Quirk, R. P.; Foster, M. D. *Macromolecules* **2005**, *38*, 5381. (b) Elkins, C. L.; Viswanathan, K.; Long, T. E. *Macromolecules* **2006**, *39*, 3132. (c) Hirao, A.; Higashihara, T.; Inoue, K. *Macromolecules* **2008**, *41*, 3579.

(9) Some examples:(a) Shohi, H.; Sawamoto, M.; Higashimura, T. *Macromolecules* **1991**, *24*, 4926. (b) Storey, R. F.; Shoemake, K. A.; Mays, J. W.; Harville, S. *J. Polym. Sci., Part A: Polym. Chem.* **1997**, *35*, 3767. (c) Jacob, S.; Majoros, I.; Kennedy, J. P. *Macromolecules* **1996**, *29*, 8631.

(10) Some examples:(a) Wiltshire, J. T.; Qiao, G. G. *Macromolecules* **2006**, *39*, 4282. (b) Trollsås, M.; Atthof, B.; Wursch, A.; Hedrick, J. L.;

Pople, J. A.; Gast, A. P. *Macromolecules* **2000**, *33*, 6423. (c) Trollsås, M.; Hedrick, J. L.; Mecerreyes, D.; Dubois, Ph.; Jérôme, R.; Ihre, H.; Hult, A. *Macromolecules* **1997**, *30*, 8508. (d) Zhao, Y.; Shuai, X.; Chen, C.; Xi, F. *Macromolecules* **2004**, *37*, 8854. (e) Hedrick, J. L.; Magbitang, T.; Connor, E. F.; Glauser, T.; Volksen, W.; Hawker, C. J.; Lee, V. Y.; Miller, R. D. *Chem.—Eur. J.* **2002**, *8*, 3309. (f) Taton, D.; Feng, X.; Gnanou, Y. *New J. Chem.* **2007**, *31*, 1097.

(11) Some examples:(a) Bazan, G. C.; Schrock, R. R. *Macromolecules* **1991**, *24*, 817. (b) Nomura, K.; Watanabe, Y.; Fujita, S.; Fujiki, M.; Otani, H. *Macromolecules* **2009**, *42*, 899. (c) Beerens, H.; Verpoort, F.; Verdonck, L. *J. Mol. Catal. A: Chem.* **2000**, *159*, 197.

(12) Some examples:(a) Bosman, A. W.; Vestberg, R.; Heumann, A.; Fréchet, J. M. J.; Hawker, C. J. *J. Am. Chem. Soc.* **2003**, *125*, 715. (b) Gao, H.; Ohno, S.; Matyjaszewski, K. *J. Am. Chem. Soc.* **2006**, *128*, 15111. (c) Gao, H.; Matyjaszewski, K. *Macromolecules* **2008**, *41*, 1118. (d) Wiltshire, J. T.; Qiao, G. G. *Macromolecules* **2008**, *41*, 623. (e) Mayadunne, R. T. A.; Jeffery, J.; Moad, G.; Rizzardo, E. *Macromolecules* **2003**, *36*, 1505. (f) Tsoukatos, T.; Pispas, S.; Hadjichristidis, N. *J. Polym. Sci., Part A: Polym. Chem.* **2001**, *39*, 320. (g) Terashima, T.; Kamigaito, M.; Baek, K.-Y.; Ando, T.; Sawamoto, M. *J. Am. Chem. Soc.* **2003**, *125*, 5288. (h) Kim, Y. H.; Ford, W. T.; Mourey, T. H. *J. Polym. Sci., Part A: Polym. Chem.* **2007**, *45*, 4623. (i) Hovestad, N. J.; van Koten, G.; Bon, S. A. F.; Haddleton, D. M. *Macromolecules* **2000**, *33*, 4048. (j) Miura, Y.; Dote, H. *J. Polym. Sci., Part A: Polym. Chem.* **2005**, *43*, 3689. (k) Johnson, J. A.; Finn, M. G.; Koberstein, J. T.; Turro, N. J. *Macromolecules* **2007**, *40*, 3589. (l) Robello, D. R.; André, A.; McCovick, T. A.; Kraus, A.; Mourey, T. H. *Macromolecules* **2002**, *35*, 9334.

(13) Some examples:(a) Xia, J.; Zhang, X.; Matyjaszewski, K. *Macromolecules* **1999**, *32*, 4482. (b) Zhang, X.; Xia, J.; Matyjaszewski, K. *Macromolecules* **2000**, *33*, 2340. (c) Gao, H.; Matyjaszewski, K. *Macromolecules* **2006**, *39*, 3154. (d) Gao, H.; Tsarevsky, N. V.; Matyjaszewski, K. *Macromolecules* **2005**, *38*, 5995. (e) Gao, H.; Matyjaszewski, K. *J. Am. Chem. Soc.* **2007**, *129*, 11828.

(14) Some examples(a) Baek, K.; Kamigaito, M.; Sawamoto, M. *Macromolecules* **2001**, *34*, 215. (b) Baek, K. Y.; Kamigaito, M.; Sawamoto, M. *J. Polym. Sci., Part A: Polym. Chem.* **2002**, *40*, 2245. (c) Terashima, T.; Ouchi, M.; Ando, T.; Kamigaito, M.; Sawamoto, M. *Macromolecules* **2007**, *40*, 3581.

(15) (a) Du, J.; Chen, Y. *Macromolecules* **2004**, *37*, 3588. (b) Du, J. Z.; Chen, Y. M. *J. Polym. Sci., Part A: Polym. Chem.* **2004**, *42*, 2263.

(16) Gao, H.; Matyjaszewski, K. *Macromolecules* **2006**, *39*, 4960.

(17) Zhang, K.; Ye, Z.; Subramanian, R. *Macromolecules* **2009**, *42*, 2313. (b) Xia, X.; Ye, Z.; Morgan, S.; Lu, J. *Macromolecules* **2010**, *43*, 4889.

(18) See two review articles:(a) Domski, G. J.; Rose, J. M.; Coates, G. W.; Bolig, A. D.; Brookhart, M. *Prog. Polym. Sci.* **2007**, *32*, 30. (b) Coates, G. W.; Hustad, P. D.; Reinartz, S. *Angew. Chem., Int. Ed.* **2002**, *41*, 2236. And see some representative examples:(c) Scollard, J. D.; McConville, D. H. *J. Am. Chem. Soc.* **1996**, *118*, 10008. (d) Baumann, R.; Davis, W. M.; Schrock, R. R. *J. Am. Chem. Soc.* **1997**, *119*, 3830. (e) Jayaratne, K. C.; Sita, L. R. *J. Am. Chem. Soc.* **2000**, *122*, 958. (f) Tian, J.; Hustad, P. D.; Coates, G. W. *J. Am. Chem. Soc.* **2001**, *123*, 5134.

(19) (a) Johnson, L. K.; Mecking, S.; Brookhart, M. *J. Am. Chem. Soc.* **1996**, *118*, 267. (b) Mecking, S.; Johnson, L. K.; Wang, L.; Brookhart, M. *J. Am. Chem. Soc.* **1998**, *120*, 888. (c) Gottfried, A. C.; Brookhart, M. *Macromolecules* **2001**, *34*, 1140. (d) Gottfried, A. C.; Brookhart, M. *Macromolecules* **2003**, *36*, 3085.

(20) Huang, H.; Niu, H.; Dong, J. *Macromolecules* **2010**, *43*, 8331.

(21) Zhang, K.; Ye, Z.; Subramanian, R. *Macromolecules* **2008**, *41*, 640.

(22) (a) Zhang, Y.; Ye, Z. *Chem. Commun.* **2008**, 1178. (b) Zhang, Y.; Ye, Z. *Macromolecules* **2008**, *41*, 6331. (c) Xu, Y.; Xiang, P.; Ye, Z.; Wang, W.-J. *Macromolecules* **2010**, *43*, 8026.

(23) (a) Morgan, S.; Ye, Z.; Zhang, K.; Subramanian, R. *Macromol. Chem. Phys.* **2008**, *209*, 2232. (b) Ye, J.; Ye, Z.; Zhu, S. *Polymer* **2008**, *49*, 3382. (c) Xiang, P.; Ye, Z.; Morgan, S.; Xia, X.; Liu, W. *Macromolecules* **2009**, *42*, 4946. (d) Morgan, S.; Ye, Z.; Subramanian, R.; Wang, W.-J.; Ulibarri, G. *Polymer* **2010**, *51*, 597. (e) Xu, Y.; Campeau, P.; Ye, Z. *Macromol. Chem. Phys.* **2011**10.1002/macp.201100020.

(24) (a) Guan, Z. B.; Cotts, P. M.; McCord, E. F.; McLain, S. J. *Science* **1999**, *283*, 2059. (b) Cotts, P. M.; Guan, Z.; McCord, E.; McLain, S. *Macromolecules* **2000**, *33*, 6945. (c) Guan, Z. *Chem.—Eur. J.* **2002**, *8*, 3086.

(25) (a) Ye, Z.; Zhu, S. *Macromolecules* **2003**, *36*, 2194. (b) Ye, Z.; AlObaidi, F.; Zhu, S. *Macromol. Chem. Phys.* **2004**, *205*, 897. (c) Ye, Z.; Li, S. *Macromol. React. Eng.* **2010**, *5*, 319.

(26) Kanaoka, S.; Sawamoto, M.; Higashimura, T. *Macromolecules* **1991**, *24*, 2309.

(27) Eschwey, H.; Burcard, W. *Polymer* **1975**, *16*, 180.

(28) Hiemenz, P. C.; Lodge, T. P. *Polymer Chemistry*, 2nd ed.; CRC Press: Boca Raton, FL, 2007.

(29) Mourey, T. H.; Turner, S. R.; Rubinstein, M.; Fréchet, J. M. J.; Hawker, C. J.; Wooley, K. L. *Macromolecules* **1992**, *25*, 2401.

(30) Lepoittevin, B.; Matmour, R.; Francis, R.; Taton, D.; Gnanou, Y. *Macromolecules* **2005**, *38*, 3120.

(31) Held, D.; Müller, A. H. E. *Macromol. Symp.* **2000**, *157*, 225.

(32) Gauthier, M.; Li, W.; Tichagwa, L. *Polymer* **1997**, *38*, 6363.

(33) Aharoni, S. M.; Crosby, C. R. I.; Walsh, E. K. *Macromolecules* **1982**, *15*, 1093.

(34) Huang, H.-M.; Liu, I.-C.; Tsiang, R. C.-C. *Polymer* **2005**, *46*, 955.